ACS Catalysis

Research Article

pubs.acs.org/acscatalysis

Exploring Meerwein–Ponndorf–Verley Reduction Chemistry for Biomass Catalysis Using a First-Principles Approach

Rajeev S. Assary,*[,†] Larry A. Curtiss,*[,†,‡] and James A. Dumesic[§]

[†]Materials Science Division and [‡]Centers for Nanoscale Materials, Argonne National Laboratory, Argonne, Illinois 60439, United States

[§]Department of Chemical & Biological Engineering, University of Wisconsin-Madison, 1415 Engineering Drive, Madison, Wisconsin 53706, United States

Supporting Information

ABSTRACT: Liquid phase catalytic hydrogenation of decomposition products of sugar molecules is challenging, but essential to produce platform chemicals and green chemicals from biomass. The Meerwein–Ponndorf–Verley (MPV) reduction chemistry is an excellent choice for the hydrogenation of keto compounds. The energy landscapes for the liquid phase catalytic hydrogenation of ethyl levulinate (EL) and furfural (FF) by Sn(IV) and Zr(IV) zeolite-like catalytic sites utilizing the hydrogen atoms from an isopropanol (IPA) solvent are explored using quantum chemical methods. The computed apparent activation free energy for the catalytic hydrogenation of EL by a Sn(IV) zeolite-like catalyst model site is (21.9 kcal/mol), which is close to the Al(III)-isopropoxide catalyzed (20.7 kcal/mol) EL hydrogenation indicating the similar efficiency of the Sn(IV) zeolite-like catalyst compared with the Al(III) catalyst used in the traditional MPV reactions. The catalytic efficiency of metal isopropoxides for the catalytic hydrogenation of EL is computed to be Al(III) > Sn(IV) > Zr(IV) in IPA solution, in agreement with experiment. Calculations were also performed with furfuryl alcohol as the source for hydrogen for the conversion of EL to γ-valerolactone using the Sn(IV) catalytic site. The barrier (22.7 kcal/mol) suggests a hydrogenation using aromatic primary alcohol as a hydrogen donor and using a Sn(IV) catalyst is feasible. In terms of reaction mechanisms, an intramolecular hydride transfer through a six membered transition state was found to be the turnover controlling transition state of liquid phase catalytic hydrogenation of carbonyl compounds considered in this study.

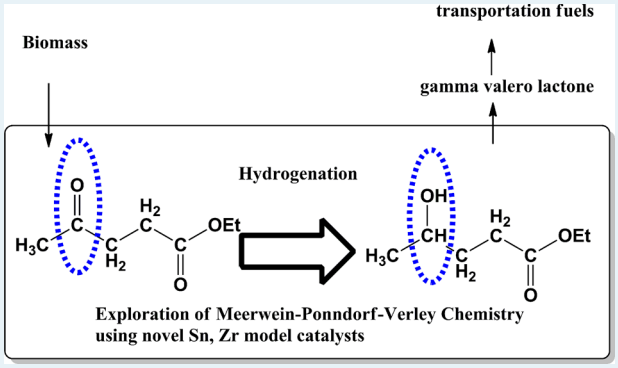

KEYWORDS: *liquid phase catalytic hydrogenation, quantum chemical studies, free energy landscapes, activation free energy barriers, aldol reactions*

1. INTRODUCTION

Biomass has the potential to become a sustainable precursor to industrial chemicals and transportation fuels, hence reducing the dependency on fossil fuels and petroleum derivatives.[1−10] Acid catalyzed dehydration is a widely used method to produce platform chemicals such as furfural (FF) predominantly from C_5 sugars, 5-hydroxymethylfurfural (HMF) from C_6 sugars, and levulinic acid/ethyl levulinate (LA/EL) from C_5 or C_6 sugars. The hydrogen content in these platform chemicals are relatively smaller than their parent sugar molecules because of the removal of water molecules, and the dehydration reactions results in the formation of chemically stable keto (-C═O) compounds (for example, removal of three water molecules from fructose and xylose gives HMF and FF, respectively). An essential transformation of these compounds to alternative fuels and desired industrial chemicals requires hydrogen and, interestingly, biomass is a potential source. One equivalent of hydrogen is required to convert FF to furfuryl alcohol (FA), a precursor of LA/EL[11,12] and for the conversion of LA to 2-hydroxy pentanoic acid (2HP), a precursor of γ-valerolactone (GVL),[13,14] as shown in Scheme 1. Potential hydrogen donors such as formic acid, lactic acid, glyceraldehyde, and ethylene glycol can also be produced as the side products of hexose decomposition[15] (acid-catalyzed dehydration or retro-aldol reactions).

Efficient catalytic processes are required to transfer the hydrogen from potential donors to platform chemicals such as HMF, FA, and LA. One of the possible routes for the hydrogenation of these keto compounds is liquid phase catalytic hydrogenation using formic acid as a hydrogen donor through homogeneous catalysis. This can be performed in solution using Pd, Rh,[16] Ru, Fe, Al, and lanthanides[17] or in the presence of salts (hydrothermal conditions). Another option is the catalytic hydrogen transfer using heterogeneous

Received: February 12, 2013
Revised: September 6, 2013
Published: October 4, 2013

Scheme 1. (top) Schematic Representation of Hydrogenation of LA or EL to 2HP or 2-Hydroxy-ethyl levulinate (2HEL) Using Isopropanol (IPA) or FA as a Hydrogen Source during the Conversion of LA/EL to GVL; (bottom) Hydrogenation of FF to FA with IPA as the Hydrogen Source

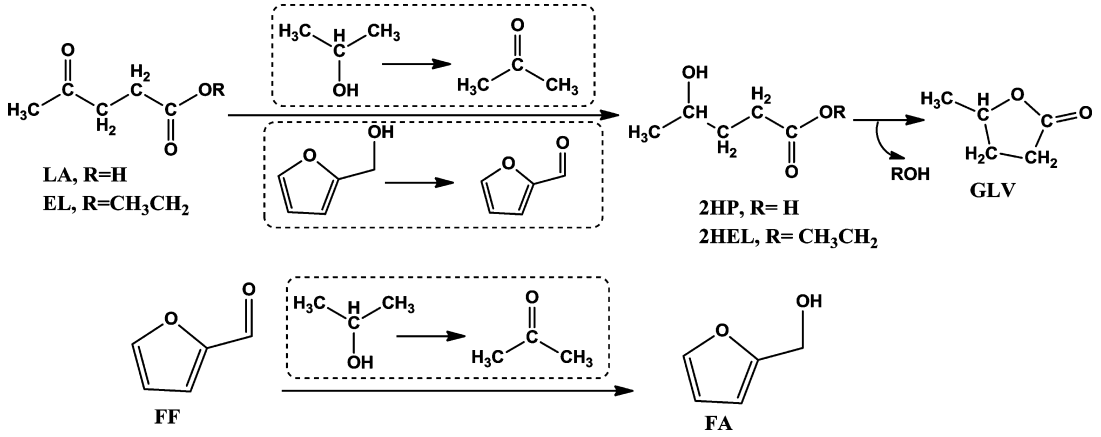

catalysts such as ZrO_2, CeO_2, and MgO along with a secondary alcohol as hydrogen transfer. In this scenario, formic acid as hydrogen donor is generally avoided because of the catalytic poisoning ability of carboxylate group.[18] Among the above-mentioned methods, heterogeneous catalysis is preferred over homogeneous catalysis involving precious metals. Also homogeneous catalysis requires high temperature, high pressure methods, which are techno-economic demanding.[19] Central to the catalysis is the involvement of a metal atom, where the binding of the substrate (for example LA or EL) and a hydrogen donor molecule (an alcohol) occurs and subsequent intermolecular hydrogen transfer resulting in the reduction of the keto group to the corresponding alcohol, similar to the Meerwein−Ponndorf−Verley (MPV) reduction reaction.

The original MPV reduction of ketones is catalyzed by a Al(III) central atom in the presence of a secondary alcohol as a hydrogen donor, and the detailed reaction mechanism is well understood.[20] The requirement of a large amount of reagents and undesired side reactions (aldol reactions) are known to be the drawbacks of MPV reduction using Al(III) species.[21] Recently, Corma and co-workers[22−24] have shown that large pore zeolites with hydrolyzed Sn or Zr active sites can reduce cyclohexanone to cyloheaxanol using the hydrogen atoms from a secondary alcohol, 2-butanol. Recently, it was also shown that the Sn-beta can be used for "one pot" conversion of glucose to HMF or LA in the presence a Brønsted acid in aqueous solutions,[25] and this is mainly due to the catalytic ability of the Lewis acid/Lewis base combination (Sn and OH, respectively) in promoting hydrogen transfer and proton abstraction.[26,27] Additionally, Dumesic and co-workers[19] have shown that the ZrO_2 can be used as an effective heterogeneous catalyst in the presence of a hydrogen donor, IPA (or any secondary alcohol) to hydrogenate LA/EL to GVL (Scheme 1). Previously, we have investigated the thermochemistry of various decomposition patterns of hexoses and cellobiose molecules to platform chemicals.[15,28−30]

Since molecular species with keto-functional groups are the major products upon the decomposition of sugars (cellobiose, hexoses, pentoses), it is essential to understand and improve upon the hydrogenation chemistry of these keto compounds using appropriate hydrogen sources. In this paper, we report on a systematic computational study of the reaction pathways for liquid phase Al(III), Sn(IV), Zr(IV) isopropoxide catalyzed hydrogenation of EL. Analogous reaction pathways are computed for hydrogenation of EL by Sn(IV), Zr(IV) on a model zeolite framework catalytic site in the presence of IPA. FF is also considered in the calculations of the reaction pathways for the Sn(IV) zeolitic site with both IPA and FA as the hydrogen source. Finally, one of the possible side reactions, aldol condensation of EL and FF, is also considered. The structures, reaction energies, and reaction barriers are used to compare catalytic properties of the different forms of the metal sites and hydrogen donor. The theoretical methods used are described in Section 2. Results for the various types of metal sites and hydrogen donors are given in Section 3.

2. COMPUTATIONAL METHODS

The computations in this paper were carried out using the B3LYP[31] and the MP2 levels of theory, which is similar to our previous work[27] where we reported a detailed mechanism for glyceraldehyde-dihydroxy acetone isomerization by a Si/Sn/Zr/Ti-beta active site. In the computations the Lewis acid metal atom is treated using CC-pVDZ-PP,[32] LANL2TZ,[33]6-31+G(d) basis sets for Sn, Zr, and Si atoms, respectively. The 6-31+G(d) basis set is used for the rest of the atoms. The B3LYP level of theory is used for gas phase geometry optimization and frequency calculations (free energy corrections at 298 K). To assess dispersion energies and basis set superposition errors a single point energy evaluation is performed at the MP2 level of theory with a combination of aug-CC-pVQZ (for Sn,[32] Zr[34]) and 6-311++G(3df,3pd) (rest of the atoms) on the geometry obtained from the density functional studies (B3LYP). Effective Core Potentials (ECP) for Sn and Zr were used to include relativistic effects in both the DFT and the MP2 calculations.[35] Detailed benchmarking of the theory used in this paper against high level G4[36] and CCSD(T) levels of theory are described elsewere,[27] which confirm the reliability of the level of calculation chosen here. Frequency calculations (B3LYP) were performed to determine whether the stationary points are minima or transition states (TS) and to provide zero point energy and free energy corrections (at 298 K, 1 atm pressure). Intrinsic reaction coordinate (IRC) calculations were also performed to confirm the existence of transition states. To account for the effects of solution environment around the catalytic active site, calculations were performed in a 2-propanol dielectric using the SMD solvation model[37] at the B3LYP level

dx.doi.org/10.1021/cs400479m | ACS Catal. 2013, 3, 2694−2704

Table 1. Computed Gas Phase Enthalpies of the Reaction (ΔH^{rxn}), Free Energies of the Reaction (ΔG^{rxn}), Enthalpies of Activation ($\Delta H^{‡}$), and Free Energies of Activation ($\Delta G^{‡}$) for the Hydrogenation of LA to 2HP Using Various Hydrogen Donors[a]

reaction	ΔH^{rxn}	ΔG^{rxn}	$\Delta H^{‡}$	$\Delta G^{‡}$
LA + formic acid →2HP + CO_2	−21.6	−18.7	26.4	40.2
	(−14.2)	(−11.3)	(28.4)	(42.3)
LA + formic acid →2-keto pentane diol + CO_2	−8.3	−6.0	32.9	46.2
	(−3.5)	(−1.2)	(34.3)	(48.3)
LA + ethanol →2HP + acetaldehyde	+2.1	+3.4	23.1	37.3
	(3.2)	(4.5)	(26.1)	(40.3)
LA + IPA →2HP + isopropanone	−0.9	+0.8	22.2	36.2
	(−0.8)	(+0.8)	(25.1)	(39.2)
LA + 2-butanol →2HP + 2-butanone	−0.5	−0.1	21.9	35.9
	(−0.6)	(−0.1)	(25.1)	(39.1)
LA + FA →2HP + FF	+0.6	+2.7	21.5	36.3
	(2.1)	(4.2)	(24.5)	(39.9)
LA + hydroxyl-ethyl-furan →2-HP + 2-acetoxy furan	+3.7	+5.0	21.2	35.9
	(4.9)	(6.2)	(25.3)	(39.8)
LA + glyceraldehyde →2HP + 2-keto-propanaldehyde	+10.6	+11.0	23.0	37.0
	(9.0)	(9.5)		
LA + ethyl lactate →2HP + 2-keto-ethyl lactate	+8.6	+8.9	22.9	36.9
	(7.2)	(7.5)		

[a]Calculated at the MP2/6-311++G(3df,3pd)//B3LYP/6-31+G(d) level of theory. Values given in the parentheses include solvation contributions. All energies are reported in kcal/mol.

of theory with the same basis sets as used for the geometry evaluations. In certain reaction steps an explicit reactant molecule is included as needed. We note that this is an approximation used to capture the solvation energy of the catalytic center, substrate molecules (for example: EL and isopropyl alcohol), and the dielectric effect from the zeolitic framework. To assess accurate binding energies of the substrate with the catalytic site (liquid phase) it is essential to perform periodic density functional studies and combined quantum mechanical/molecular mechanical studies, which is beyond the scope of this manuscript.

The free energy of the reaction (ΔG^{rxn}), enthalpy of reaction (ΔH^{rxn}), and the free energy/enthalpy of activation ($\Delta G^{‡}$/$\Delta H^{‡}$) reported in this paper include the MP2 single point energy and free energy/enthalpy corrections and solvation energies from the B3LYP level of theory unless mentioned otherwise. Both free energy and enthalpy profiles in solutions for all reaction pathways are given. The calculations for this investigation were done using Gaussian 09.[38]

To understand the efficiency (or turn over frequency) of the catalytic reactions from the free energy landscapes, recently Kozuch[39−41] and co-workers have applied an energetic span model, where both turn over frequency-determining transition state (TDTS) and turnover frequency-determining intermediates (TDI) are located from the energy profile. The TDTS-TDI energy difference and the reaction driving force define the energetic span (δE). Details can be found in refs 38 and 39, and references therein) of the catalytic cycle. Also, whenever TDTS appears after the TDI, the δE is the difference between these two states. If the TDI appears after the TDTS, a correction is required that includes the addition of free energy to form the TDI.[40] In our calculations, the correction is negligible (less than a kcal/mol) and therefore not included. The computed δE serves as the apparent activation free energy of the catalytic cycle, which is computed and discussed in all free energy landscapes.[42,43]

3. RESULTS AND DISCUSSIONS

3.1. Catalyst Free Inter- and Intramolecular Hydrogen Transfer. To understand the reaction energies and reaction barriers for the direct hydrogenation of LA by various the hydrogen donors, we have carried out computations without a catalyst. We have considered formic acid, ethanol, IPA, 2-butanol, FA, 2-hydroxy-ethyl-furan, glyceraldehyde, and ethyl lactate as potential hydrogen donors for the reduction of the keto group of LA.

The enthalpies of the reaction (ΔH^{rxn}), free energies of the reaction (ΔG^{rxn}), enthalpies of activation ($\Delta H^{‡}$), and free energies of activation ($\Delta G^{‡}$) were computed (both gas phase and solution phase) and summarized in Table 1. The enthalpy barriers computed for the reduction of the keto group by formic acid and carboxylate group of LA are 26.4 kcal/mol ($\Delta G^{‡}$ = 40.2 kcal/mol) and 32.9 kcal/mol ($\Delta G^{‡}$ = 46.2 kcal/mol), respectively. The computed energy profiles are similar for the hydrogenation of EL by formic acid. Based on the computed reaction energetics (barriers and free energies) presented in Table 1, it is evident that the hydrogen donors such as formic acid, 2-butanol, and IPA are more likely candidates than the primary alcohols (ethanol, FA, and hydroxy ethyl furan), glyceraldehyde, and ethyl lactate in hydrogenation reactions. Additionally the energetics for hydrogenation reactions are quantitatively similar regardless of the solvation energy for the uncatalyzed reactions.

The enthalpies of activation required for the direct hydrogen transfer (Scheme 2, *left*) are in the range of 22−26 kcal/mol (Gibbs free energies of activation are in the range of 30 to 40 kcal/mol). The direct hydrogen transfer occurs through a six-membered transition state, shown in Scheme 2 (*left*). Also, EL could undergo intramolecular hydrogen transfer (Scheme 2, and Supporting Information, Figure S5) to form GVL and acetaldehyde (*right*). However, this process is endothermic and requires a significant activation barriers ($\Delta H^{‡}$ =57.6, $\Delta G^{‡}$= 63.1 kcal/mol). The relatively large reaction barrier for intramolecular hydrogen transfer suggests that, in the presence

dx.doi.org/10.1021/cs400479m | ACS Catal. 2013, 3, 2694−2704

Scheme 2. Schematic Representation of the Transition State of Hydrogen Transfer[a]

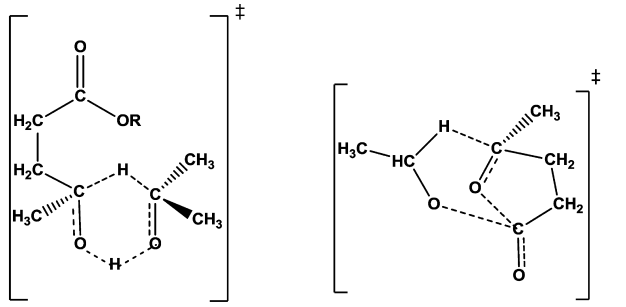

Inter-molecular hydrogen transfer to EL from isopropanol

Intramolecular hydrogen transfer of EL

[a] *Left*: inter-molecular hydrogen transfer between EL and IPA to form 2HEL. *Right*: intra-molecular hydrogen transfer in EL to form GVL and acetaldehyde.

of hydrogen donors (solvents such as secondary alcohols), intermolecular hydrogen transfer is preferred.

3.2. MPV Reduction of EL by Al(III), Sn(IV), Zr(IV)-Isopropoxides. Previously, Cohen et al. have investigated a detailed reaction mechanism of the MPV reaction for ketones catalyzed by Al(III) isopropoxide, and an intermolecular hydrogen transfer mechanism was postulated.[20] We have considered a similar initial reaction mechanism for the hydrogenation of EL catalyzed by Al(III) isopropoxide in IPA solution. The detailed free energy and enthalpy profile is shown in Figure 1.

From the Figure 1, the initial step shown is the exothermic (and exergonic) binding (A→B) of EL with the catalyst in the solution. It is likely that the Al(III) propoxide is coordinated with a solvent molecule (IPA) and the substrate, EL replaces the solvent molecule to form the intermediate B (the detailed Gibbs free energies for the formation of Intermediate B in the presence of an explicit solvent molecule is also presented in the Supporting Information, Figure S1). This is followed by the hydride transfer from the keto carbon of the isopropoxide to the keto carbon of the EL (B→D) through a transition state **C**. In solution the ketone (isopropanone) will be replaced by the solvent molecule, IPA from intermediate D to form the complex E. This process (D→E) is both exergonic and exothermic, and the intermediate E is the lowest energy intermediate. The release of the 2HEL (E→G) requires a proton from the solvent molecule (since no acidic protons are available). The protonation occurs via a transition state F that leads to the formation of 2HEL and an isopropanone molecule (G).

Analyzing the free energy profile in the Figure 1, the TDTS is the hydride shift (B→C) and the TDI is the intermediate E. Therefore, the activation enthalpy for this reaction is the barrier

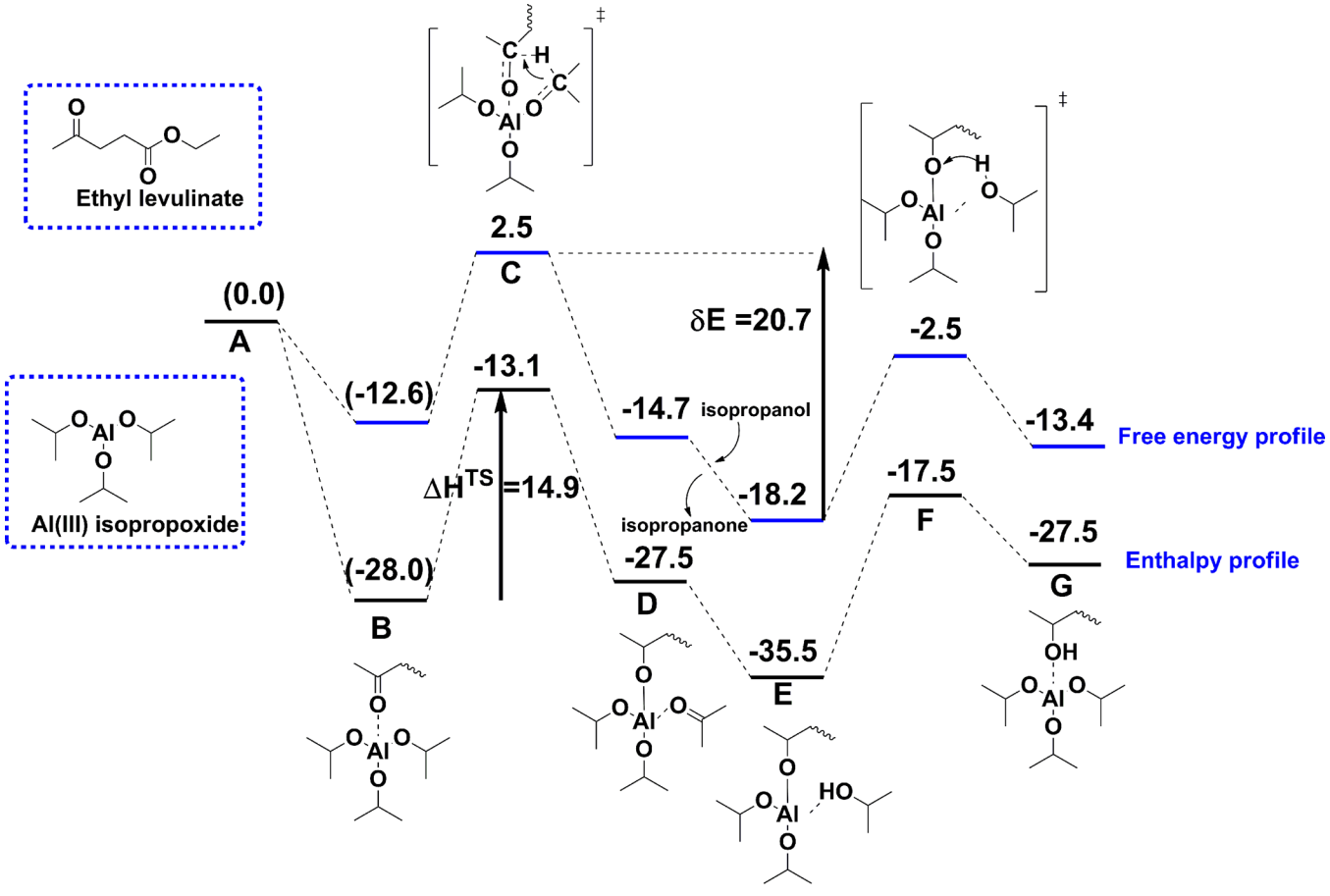

Figure 1. Computed free energy and enthalpy profiles (MP2 level) for the liquid phase hydrogenation of EL to 2HEL by Al(III) isopropoxide in IPA medium. The free energy/enthalpy corrections and solvation energies were computed at the B3LYP level of theory. All energies are referenced to Al(III) isopropoxide and EL in solution (A) and reported in kcal/mol. Note that an implicit solvation model for IPA is used in all steps, and an explicit IPA molecule is added at step D→E, in addition to the implicit solvation model.

dx.doi.org/10.1021/cs400479m | *ACS Catal.* 2013, 3, 2694−2704

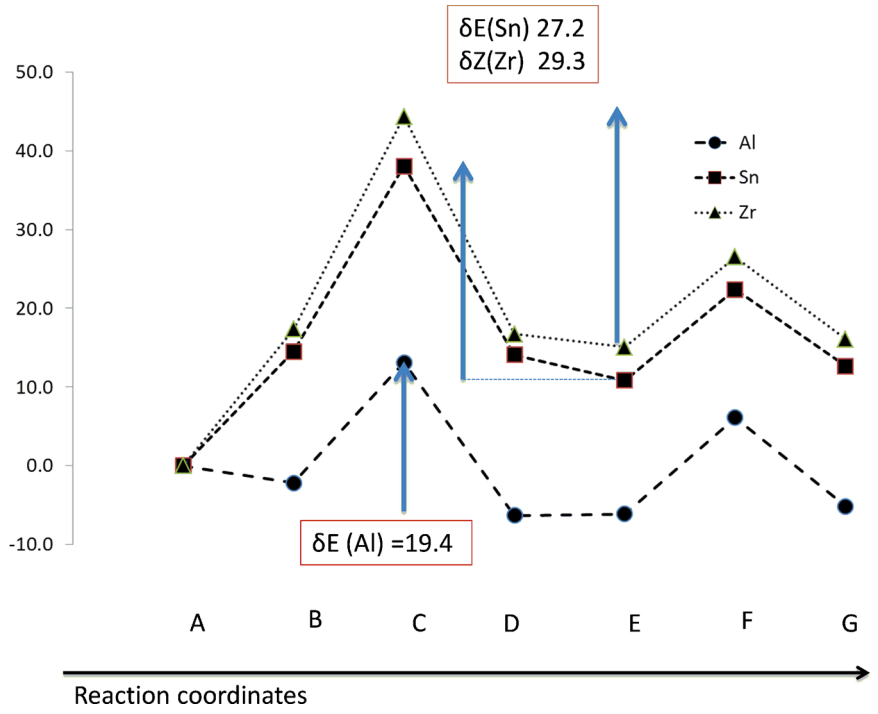

Figure 2. Computed (B3LYP) free energy profiles for the catalytic hydrogenation of EL to 2HEL by Al(III), Sn(IV), and Zr(IV) isopropoxide in an IPA dielectric medium. The reaction coordinates A to G are the same as in Figure 1. The energies (MP2 level) for intermediates are also given in Supporting Information, Table S1.

for the hydride shift, which is 14.9 kcal/mol, in good agreement with previous experimental and theoretical DFT studies by Cohen et al.[20] for other ketones. Importantly, based on the energetic span model, the computed apparent activation free energy barrier (δE) is 20.7 kcal/mol at the MP2 level of theory (the contribution from ΔG_{rxn} for the reaction from B to G is negligible, See Figure 1). At the B3LYP level of theory, the computed value for δE is 19.4 kcal/mol, which is in excellent agreement with the high-level MP2 calculations (20.7 kcal/mol, See Figure 1). (See Supporting Information, Figure S3 for the comparison between the MP2 vs DFT free energy profiles).

In addition to the Al(III)-isopropoxide, experimentally it is shown that both Sn and Zr isoproxides can be used in the MPV hydrogenation of aldehydes.[44,45] Similar to the Al(III)-catalyzed liquid phase hydrogenation of EL, computations were also performed using the Sn (IV) and Zr(IV)-isoproxide catalysts in IPA medium to understand the free energy landscape and assess the relative catalytic ability of these isopropoxides. In Scheme 2, the computed free energy profiles for Sn(IV)/Zr(IV) isopropoxide in solution is compared with that of the Al(III)-catalyzed reaction. A noticeable difference is the energetics for the formation of the initial binding complex between the metal center and the EL. In terms of free energy, the binding energy of Sn(IV) and Zr(IV) with EL is endergonic compared to Al(III), where the binding is exergonic. In terms of enthalpy, the binding of EL is exothermic. Qualitatively, the free energy profile for the Sn(IV) and Zr(IV) catalyzed hydrogenation of EL is similar to that of Al(III), as shown in Figure 2. This suggests that we can employ the energetic span model for computing the apparent activation free energy barriers (δE) for the reactions. From Figure 2, the computed δE values for Al(III), Sn(IV), and Zr(IV) catalyzed reactions are 19.4, 27.2, and 29.3 kcal/mol, respectively. This clearly indicates the superior catalytic efficiency of Al(III) compared to Sn(IV) or Zr(IV) in IPA solutions. Additionally, the computed free energy profile shown in Figure 2 also indicates that the initial binding of the EL is likely the key factor behind the superior catalytic performance of Al(III) compared to the Sn(IV) or Zr(IV) isopropoxides.

The above computations reveal the energy landscape for a known catalyst, Al(III) isopropoxide, for our desired chemical reaction (hydrogenation of the keto group), and the computed energetics can be taken as a reference for the study of Sn(IV), Zr(IV) zeolitic catalyst models employed in the following sections. The calculations suggest that catalytic active sites with strong binding similar to that of Al(III) should have superior performance for the hydrogenation of aldehydes or ketones.

3.3. Hydrogenation of LA by Sn/Zr Zeolitic Models Using IPA as the Hydrogen Source. Previously, Boronat et al.[22] have performed theoretical studies to explain the detailed energetics of Sn/Zr-beta active sites in catalyzing the hydrogenation of cyclohexanone to cyclohexanol using the hydrogen atoms from 2-butanol. The catalytic ability is predominantly due to the presence of the central metal atom, which acts as a Lewis acid and the hydroxyl ligand attached to the metal atom acts as a Lewis base. Similar to this, recently, we have also carried out theoretical studies of glyceraldehyde-dihydroxy acetone and glucose-fructose isomerization reactions (combined experimental and theoretical studies) using Sn, Ti, and Zr active site models.[27,46] Similar to the above studies, we have considered a tetrahedral metal site, coordinated with three $-OSiH_3$ groups and one $-OH$ group (in a dielectric medium) as the catalyst model, which was found to be sufficient enough to explain the relative binding of the substrates, energy landscapes, and the activation enthalpy of the glucose-fructose isomerization reaction.[46] We note that to compute the accurate binding energies and the influence of the catalytic support/

dx.doi.org/10.1021/cs400479m | ACS Catal. 2013, 3, 2694−2704

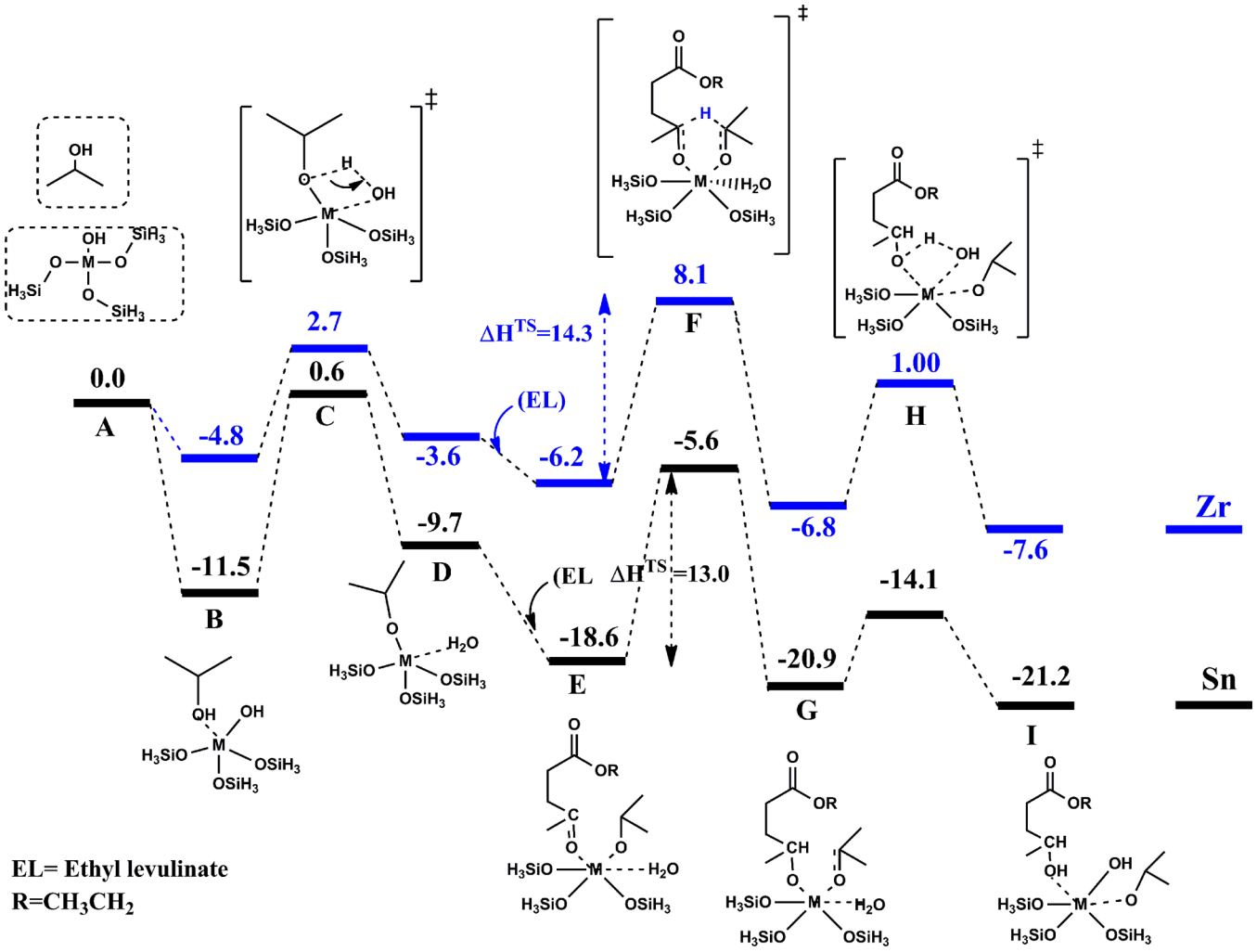

Figure 3. Computed enthalpy profile (MP2 level) for the liquid phase hydrogenation of EL to 2HEL by Sn(IV) and Zr(IV) model zeolitic catalysts using IPA as the hydrogen donor in IPA solvent medium. The enthalpy corrections (298 K, 1 atm pressure) and solvation energies were computed at the B3LYP level of theory. All energies are reported in kcal/mol. Note that an implicit solvation model for IPA is used in all steps; an explicit IPA is added at step A→C and an explicit EL molecule is added at Step D→E.

framework confinement on catalysis it is essential to perform larger zeolite/cluster model or periodic calculations.[47]

Thus, the cluster model considered for this study can be a mimic of the active site of a novel zeolite-like catalyst. Because of the presence of carboxylate group, LA is not an ideal starting compound for the reduction using metal ions due to the strong affinity of carboxylate functional group toward the metal ion. Therefore EL is chosen to study the relative catalytic ability of the Sn and Zr model catalysts in IPA. The detailed enthalpy and free energy profiles are shown in Figures 3 and 4 respectively. The reaction sequence proceeds via three key reaction sequence steps (Figure 2) as follows.

(a) Deprotonation of IPA by the Lewis base (−OH): A→D.

(b) Intermolecular hydride transfer from the carbon with the activated oxygen atom: D→G.

(c) Protonation of alkoxy group by the water ligand: G→I.

In Figures 3 and 4, all energies are presented with respect to the energies of isolated species in solution (A). An implicit solvent model is used as an approximation to account for the effect of the zeolitic framework. Based on the enthalpy profile for the Sn(IV) catalyzed hydrogenation (Figure 3), the binding of IPA with the central metal atom is exothermic to form B (−11.5 kcal/mol). The Lewis base, −OH, then abstracts the proton from the hydroxyl group of IPA resulting in the formation of complex (**D**, −9.7 kcal/mol) with a new Sn−O bond (**B**→**D**). This process occurs via transition state **C** (0.6 kcal/mol) and requires an enthalpy of activation of 12.1 kcal/mol from B. The next step is the binding of EL to the complex **D** to form **E** (−18.6 kcal/mol). Note that, it is also likely that another solvent molecule (IPA) binds to the active site. (The binding of another IPA to the complex **D** is also exothermic, and has an energy −16.9 kcal/mol with respect to A). Formation of the complex is a key intermediate, considered as the precursor complex to the hydrogen transfer. It is likely that in IPA solution, a catalyst active site may make various complexes with IPA and EL prior to the formation of Intermediate E. (See Supporting Information, Figure S4). Upon the formation of **E**, the transfer of a hydride from the IPA to the keto carbon of the EL occurs via a six-membered transition state (**F**, −5.6 kcal/mol). The activation enthalpy required for this process is 13.0 kcal/mol. A complete transfer of hydrogen from IPA to EL (**E**→**G**) results in the formation of **G** (−20.9 kcal/mol). The formation of the 2HEL-catalyst (**I**, −21.2 kcal/mol) complex occurs by the proton transfer (**G**→**H**) from the water ligand to the Sn−O_{EL} bond. This requires a relatively smaller enthalpy of activation.

dx.doi.org/10.1021/cs400479m | ACS Catal. 2013, 3, 2694−2704

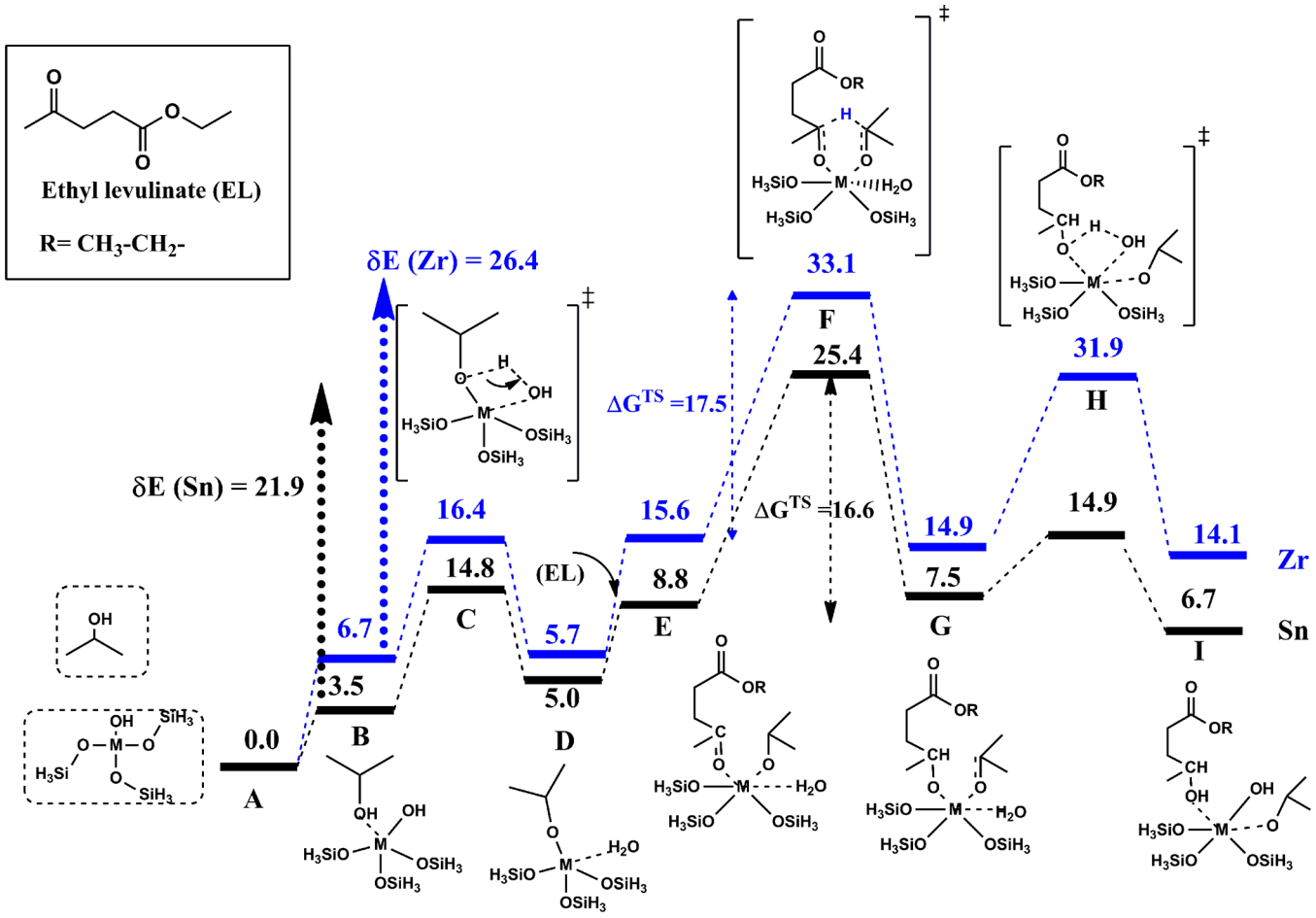

Figure 4. Computed free energy profile (MP2) for the liquid phase hydrogenation of EL to 2HEL by Sn(IV) and Zr(IV) model catalyst using IPA as the hydrogen donor in IPA solvent medium. The free energy corrections (298 K, 1 atm pressure) and solvation energies were computed at the B3LYP level of theory. All energies are reported in kcal/mol. Note that an implicit solvation model for IPA is used in all steps; an explicit IPA is included at step A→B, and an explicit EL molecule is added at Step D→E.

The enthalpy profile of a Zr (IV) zeolite model also shows a similarly shaped enthalpy profile as the Sn (IV) for the hydrogenation of EL (Figure 3). One of the notable differences is that the binding of EL to the central metal ions is not as exothermic as in the Sn (IV) site in solution. This is mainly due to the stability of Zr (IV) in solution by the IPA molecules. The key step of hydride transfer (E→F) catalyzed by the Zr-site requires an enthalpy of activation (true barrier) of 14.3 kcal/mol. Based on the free energy profile (Figure 4), it can be seen that the highest point in the free energy surface is the transition state corresponding to the hydride transfer, and it is energetically higher by 7.6 kcal/mol than the corresponding point for the Sn-catalyzed reaction, indicating the rate of hydrogenation is likely lower in the Zr(IV) catalyzed reaction than in the Sn(IV)-catalyzed reaction in solution. The detailed free energy profile for the gas phase hydrogenation of EL by Sn (IV) and Zr (IV) is computed and presented in Supporting Information, Figure S6, where Zr(IV) was found as the most efficient catalyst than the Sn(IV) in the gas phase. This information suggests that a higher catalytic activity can be expected for a Zr-based catalyst if confined to a small pore. Given that the Zr(IV) cation is located in a larger pore or as a cluster in liquid medium, Zr(IV) will be stabilized by solvation from the medium because of its relatively higher charge density than that of the Sn(IV), hence the decreased catalytic activity for liquid phase hydrogenation.

In solution, by using the energetic span model (Figure 4), the apparent free energy of activation (δE) is computed for both Sn(IV) and Zr(IV) catalyzed hydrogenation. We consider the energy span from the lowest energy intermediate B (the catalyst makes an initial complex with IPA in IPA, therefore B represents the most likely form of the catalyst active site model in the IPA medium) to the transition state (F, TDTS). The computed (δE) is also shown in Figure 4. It is 21.9 and 26.4 kcal/mol, respectively, for the Sn(IV) and Zr(IV) catalyzed hydrogenation of EL to 2HEL. The apparent free energy barrier (δE) clearly suggests that Sn(IV) is relatively more efficient in catalyzing the hydrogenation of EL compared to Zr(IV) in solution. Additionally the computed energetic span (δE = 21.9 kcal/mol) for the Sn(IV) zeolitic model is close to Al(III) isopropoxide (δE = 20.7 kcal/mol) suggesting that the Sn(IV) zeolitic site has the potential for a hydrogenation catalyst. We speculate that such a Sn(IV) or Zr(IV) site can be incorporated into likely supports such as niobia, zirconia, or silica to create a potential catalyst for the hydrogenation of keto compounds obtained from the decomposition of sugar molecules. We note that comprehensive experimental and theoretical studies are essential to establish this.

dx.doi.org/10.1021/cs400479m | ACS Catal. 2013, 3, 2694−2704

3.4. Hydrogenation of FF by Sn(IV) Catalyst-Model Using IPA as the Hydrogen Source. In addition to energetics of liquid phase catalytic hydrogenation of EL obtained from cellulose, hydrogenation of FF obtained from hemicellulose is also addressed here. The hydrogenation of FF to FA is a useful process, since FA can be a potential precursor to LA[11,12] and polymers.[48] Having understood the energy profile for the reduction of EL using Sn(IV) and Zr(IV) catalytic sites we focused on the hydrogenation of FF to FA using the hydrogen atoms from solvent IPA. Calculations were carried out to understand the hydrogenation of FF to FAL similar to the hydrogenation of LA in section 3.2. The hydrogenation reaction of FF by IPA is an exothermic reaction, and the enthalpy of activation for an uncatalyzed reaction is 21.2 kcal/mol. For the Sn(IV) catalyzed reaction, the computed reaction steps and energy profile are very similar for both hydrogenation processes. The computed enthalpies and free energies of steps A to I are tabulated in Table 2.

Table 2. Computed Relative Enthalpies (ΔH) and Free Energies (ΔG) of Various Intermediates for the Hydrogenation of FF to FA Catalyzed by Sn(IV) Model Catalyst in an IPA Solution[a]

reaction step	ΔH	ΔG
A	0.0	0.0
B	−11.5	+3.5
C (TS)	+0.6	14.8
D	−9.7	+5.0
E	−20.0	+5.1
F (TS)	−6.8	+21.7 (TDTS)
G	−23.6	+0.8 (TDI)
H (TS)	−14.5	+11.8
I	−22.0	+2.6

[a]Calculated at the MP2 level of theory. The free energy/enthalpy corrections and the solvation energies were computed at the B3LYP level of theory. All reaction steps (A–I) are conceptually equivalent to that of the Sn(IV)-catalyzed hydrogenation of EL shown in Figures 3 and 4. According to the energetics span model, the computed δE = 20.5 kcal/mol (energy difference between the intermediates G and F). All energies are reported in kcal/mol.

Similar to the hydrogenation of EL, the hydrogen transfer step was computed to be the rate-limiting step for the hydrogenation of FF using IPA as the hydrogen source. The computed activation enthalpy for the hydrogen transfer (E→F) is 13.2 kcal/mol. According to the energetic span model, the computed apparent activation free energy (δE) is 20.5 kcal/mol, very similar to hydrogenation of EL by Sn(IV) in the presence of IPA.

3.5. Hydrogenation of EL by Sn(IV) Catalyst-Model Using FA as the Hydrogen Source. So far, we have carried out calculations for the catalytic hydrogenation of EL using hydrogen from IPA, which is not a direct derivative of biomass. Since FA is the precursor of LA/EL, it is useful to understand the energetics of catalytic hydrogenation by utilizing hydrogen atoms from the FA itself to hydrogenate LA/EL. Additionally the process can be treated as an example of aromatic primary alcohol as a hydrogen donor.

The computed free energy/enthalpy profile for the Sn(IV)-catalyzed conversion of EL to 2HEL using the hydrogen atoms from FA is shown in Figure 5. The landscape of the enthalpy profile is found to be very similar to that when IPA was used as the solvent. The initial binding of FA to the central metal ion is exothermic (−12.5 kcal/mol), and the rate-determining hydride transfer requires an enthalpy of activation of 15.7 kcal/mol (intrinsic, process E→G). The computed apparent free energy barrier for this reaction (δE) is 22.7 kcal/mol (shown in Figure 5), which is marginally higher than when IPA is used as the hydrogen donor (δE = 20.7 kcal/mol).

The free energy profile also indicates that the FA→ FF is a thermodynamically uphill reaction (for B→ I, the ΔG = +3.4 kcal/mol). Considering the formation of GLV from 2HEL is thermodynamically downhill, the gain in energy can compensate the small energy penalty during the conversion of FA to FF if tandem catalysis can be achieved. Therefore, the proposal of using FA as a potential hydrogen donor for the conversion of EL to GVL can be justified.

One of the possible undesired reaction during the MPV reaction is the aldol formation between the alcohol and the ketone. Importantly, the aldol formation chemistry often practiced to combine the platform chemicals (C_4–C_6) to make longer chain alkanes (C_{10} alkanes). An example is the aldol reaction between EL and FF to make C_{10} species in the presence of bases.[49] Because of Lewis basicity of the −OH group attached to the Sn(IV) catalyst, we propose that the catalyst has the potential to mediate the aldol condensation. To understand the energy landscape of such a process, we have computed a detailed free energy/enthalpy profile for the aldol formation that is presented in Figure 6. The reaction sequence is initiated by the exothermic binding of the keto group of the EL to the central metal atom, Sn(IV) (**A→B**, −10.5 kcal/mol). The basic −OH group (serves as a Lewis base) abstracts the proton of the CH_3 group, alpha to the keto group of EL, to produce a carbanion and water ligand (**D**). The computed enthalpy of activation required to cross this barrier (**B→C**) is 24.1 kcal/mol. It is noteworthy that the proton abstraction process (**B→D**) is endothermic by 12.7 kcal/mol. Binding of FF to the intermediate **D** leads to complex E (−6.2 kcal/mol). Upon binding, the carbon–carbon bond formation occurs, which results in the formation of a C_{10} species coordinated with the metal ion (**F**, −24.2 kcal/mol). This process (**E→F, −18** kcal/mol) is very exothermic and barrierless. A proton transfer from the water ligand to the Sn–O bond leads to the formation of an aldol (**G**). Noticeably, the aldol binds strongly with the central metal ion, compared to 2HEL or FA, suggesting energy is required to remove the aldol product from the catalytic site to regenerate the catalyst.

Based on the free energy profile (Figure 6) the apparent activation free energy (δE) for the aldol reaction is 28 kcal/mol, relatively larger than the catalytic liquid phase hydrogenation (~20 kcal/mol) indicating that the aldol condensation may require a higher temperature than the hydrogenation process.

4. CONCLUSIONS

In this paper, we report on a quantum chemical investigation of the energetics and structures of Meerwein–Ponndorf–Verley (MPV) hydrogenation of EL catalyzed by Al(III), Sn(IV), and, Zr(IV) zeolitic-like catalysts. This MPV reaction is very selective to the keto functional group and therefore offers an excellent option for the liquid phase catalytic hydrogenation of biomass derivatives. Initially, we have computed the thermodynamic profile for the MPV hydrogenation of EL using conventional catalysts such Al(III), Sn(IV), and Zr(IV) isopropoxides in IPA. We have extended these studies by using a Sn (IV)/ Zr (IV)-cluster model for a zeolite site, which

dx.doi.org/10.1021/cs400479m | ACS Catal. 2013, 3, 2694–2704

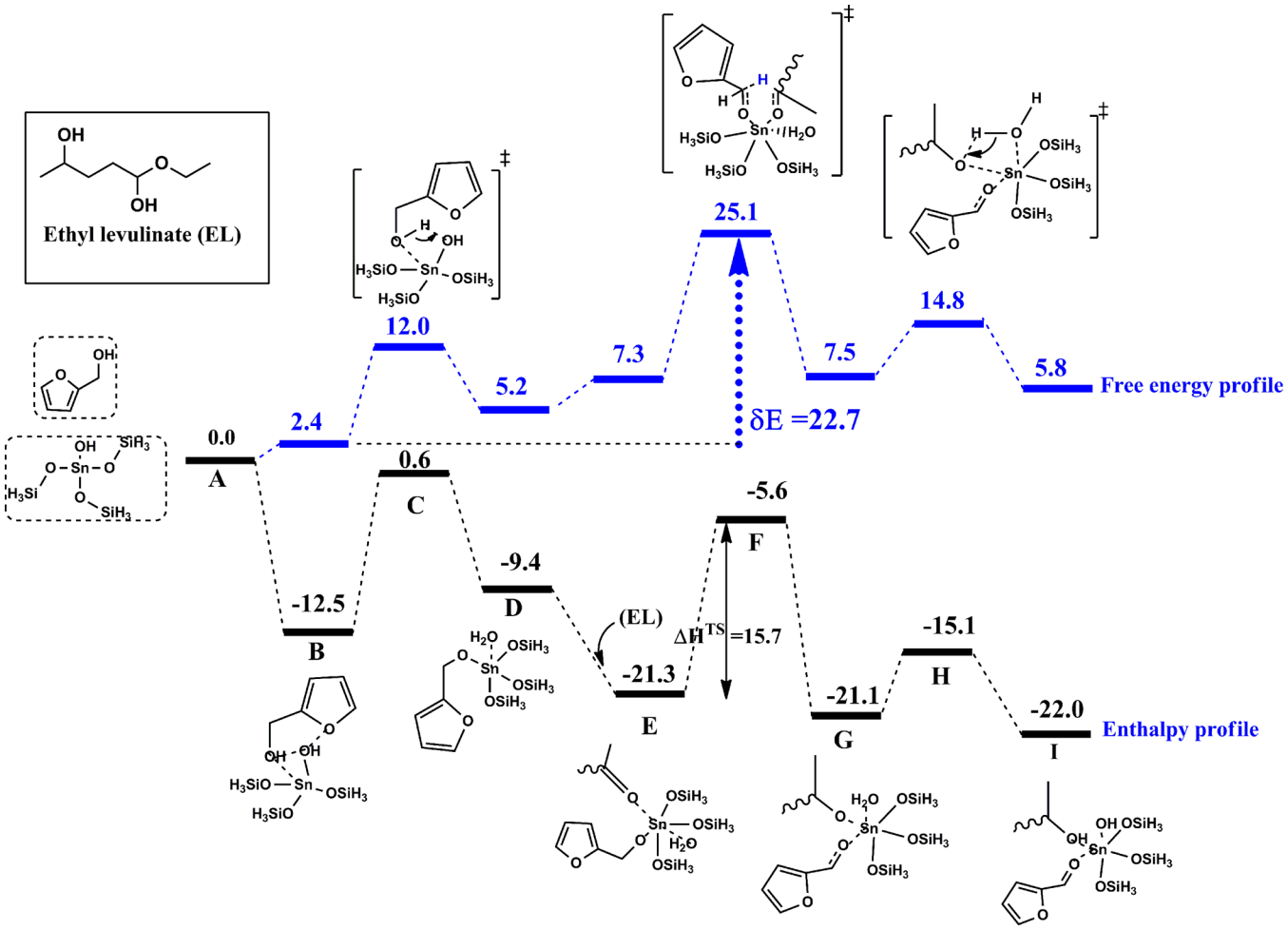

Figure 5. Computed free energy and enthalpy profiles (MP2) for the liquid-phase hydrogenation of EL to 2HEL by a Sn(IV) zeolite-like catalyst using FA as the hydrogen donor. The free energy/enthalpy corrections and the solvation energies were computed at the B3LYP level of theory. All energies are reported in kcal/mol. Note that an implicit solvation model (IPA is used as the implicit model because of lack of available solvation models for FA in Gaussian 09 software) is used in all steps; an explicit FA is included at step A→B and an explicit EL molecule is added at Step D→E.

is similar to that of the active site of Sn/Zr-beta. The computations were aimed at understanding the thermodynamic landscapes of catalytic hydrogenation of EL, FF, and possible side reaction such as aldol condensation. On the basis of the detailed structural and energy profiles investigated here, the following conclusions can be drawn from the study.

(1) The computed apparent activation free energies for the liquid phase hydrogenation of EL by Al(III), Sn(IV), and Zr(IV)-isopropoxides are 19.4, 27.2, and 29.3 kcal/mol, respectively, at the B3LYP level of theory. The computed apparent activation free energy for the Al(III) catalyzed hydrogenation is 21.7 kcal/mol at the MP2 level of theory indicating that the B3LYP and MP2 levels theory are consistent for computing the apparent activation barriers, although B3LYP underestimates the actual reaction energies. Compared to Sn(IV) and Zr(IV) isopropoxide, the binding of the substrate (EL) is significantly more exergonic with the Al(III) and is the reason that Al is more favorable for this reaction.

(2) Calculations using a cluster model, similar to the Sn-beta zeolite active site, were also performed for the catalytic hydrogenation of EL and FF in the presence of a hydrogen donor such as IPA or FA. The computed activation free energy barrier for the Sn(IV)-catalyzed reaction is 21.9 kcal/mol, which is comparable with the Al(III) isopropoxide catalyzed hydrogenation suggesting that the a zeolite-like Sn(IV) catalyst has a potential role as a hydrogenation catalyst. The computed activation free energy for the same process catalyzed by the Zr(IV) catalyst model is 26.4 kcal/mol indicating that the efficiency of Zr(IV) may be lower than the Sn(IV) for hydrogenation of EL, which is likely due to the lower Lewis acidity of Zr(IV) compared to that of Sn(IV) in solution.

(3) The basicity of the OH-group of the Sn(IV) cluster model can be utilized to condense EL and FF to form aldol, a potential precursor to long chain hydrocarbons. The computed apparent activation free energy is 28 kcal/mol, which is relatively larger than the catalytic hydrogenation (~20 kcal/mol) indicating that the aldol condensation may require a higher temperature than the hydrogenation process.

Our studies using the zeolite-like cluster model reveals the activity of the Sn(IV)/Zr(IV)-sites for the hydrogenation of keto compounds provided a hydrogen donor, such as IPA or FA, is present. Future studies are required to improve the binding domain of the catalyst for stronger binding of hydrogen donors and keto-substrates similar to that of Al(III)-isoproxide, which may improve catalytic activity. These studies highlight the need for bifunctional, size selective catalysts for the

dx.doi.org/10.1021/cs400479m | ACS Catal. 2013, 3, 2694−2704

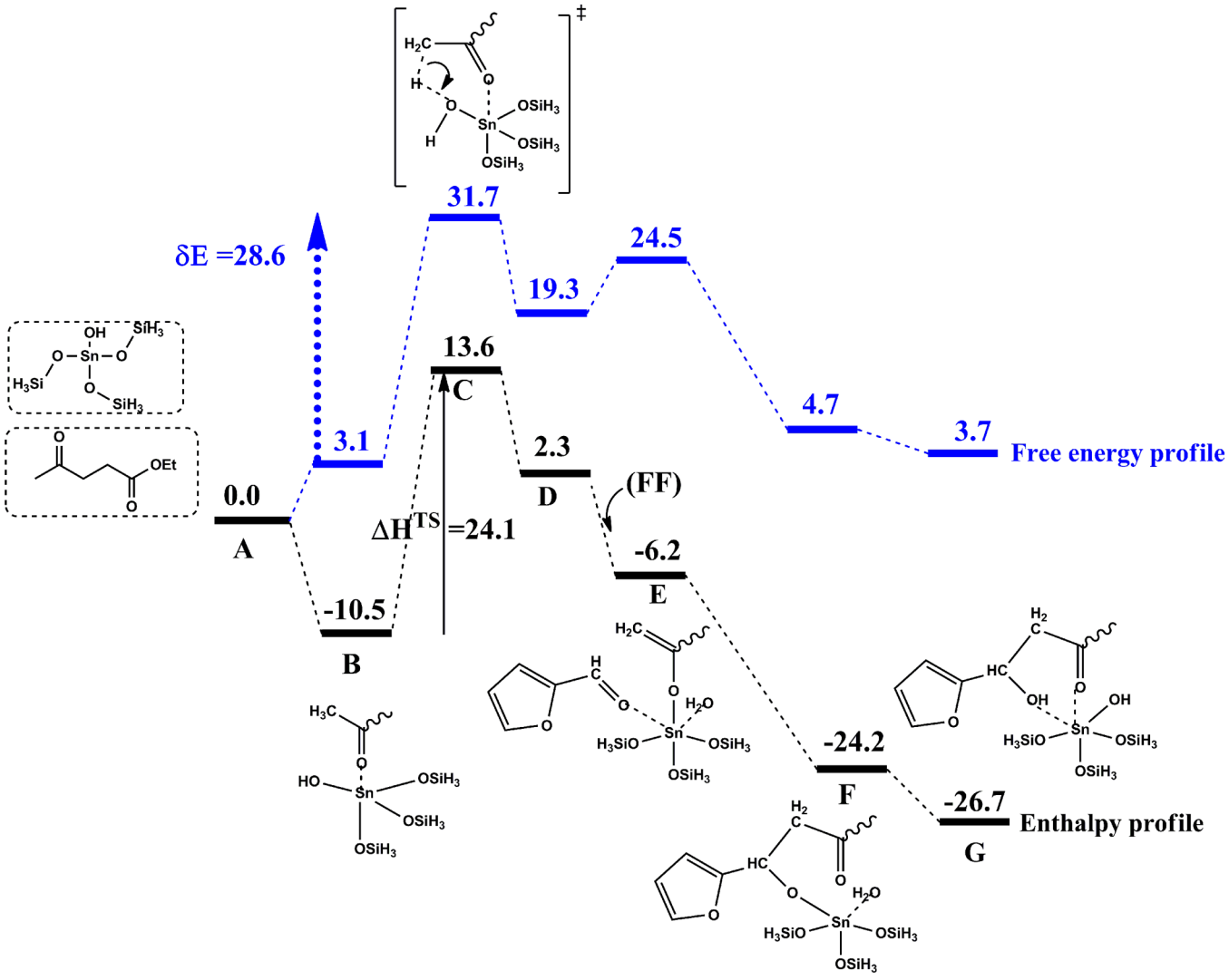

Figure 6. Computed free energy and enthalpy profiles (MP2) for the aldol reaction between EL and FF using a Sn(IV) zeolite-like catalyst in solution. All energies are reported in kcal/mol. Note that an implicit solvation model (IPA) is used in all steps; an explicit EL is included at step A→B and an explicit FF molecule is added at step D→E.

hydrogenation of keto compounds that are produced from the acid-catalyzed decomposition of sugar molecules. On the basis of our study, we envision that large pore Sn/Zr zeolites or nanobowls with appropriate binding and catalytic domains would be potential candidates for liquid phase catalytic hydrogenation of keto compounds.

■ ASSOCIATED CONTENT

Supporting Information

Computed free energies for the formation of the All(III) catalytic active site (Figure S1), free energy profile for the concerted proton coupled hydride transfer between IPA and EL catalyzed by Al(III) isopropoxide (Figure S2), comparison of computed B3LYP and MP2 free energy profiles (Figure S3), likely precursor complexes between Sn(IV) zeolitic site, IPA, and EL (Figure S4), computed transition state structure for the intramoleculear hydrogen shift (Figure S5), MP2 energies associated with Figure 2 (Table S1), and the computed gas phase free energy profile for the gas phase hydrogenation of EL by IPA molecule catalyzed by the Sn(IV) and Zr(IV) zeolitic site (Figure S6). This material is available free of charge via the Internet at http://pubs.acs.org.

■ AUTHOR INFORMATION

Corresponding Authors

*E-mail: assary@anl.gov. Phone: 630-252-7020. Fax: 630-252-9555.

*E-mail: curtiss@anl.gov. Phone: 630-252-7380. Fax: 630-252-9555.

Notes

The authors declare no competing financial interest.

■ ACKNOWLEDGMENTS

This work was supported by the U.S. Department of Energy under Contract DE-AC0206CH11357. This material is based upon work supported as part of the Institute for Atom-efficient Chemical Transformations (IACT), an Energy Frontier Research Center funded by the U.S. Department of Energy, Office of Science, and Office of Basic Energy Sciences. We gratefully acknowledge the computing resources provided on "Fusion", a 320-node computing cluster operated by the Laboratory Computing Resource Center at Argonne National Laboratory . Use of the Center for Nanoscale Materials was supported by the U.S. Department of Energy, Office of Science,

Office of Basic Energy Sciences, under Contract No. DE-AC02-06CH11357. This research used resources of the National Energy Research Scientific Computing Center (NERSC), which is supported by the Office of Science of the U.S. Department of Energy under Contract No. DE-AC02-05CH11231.

REFERENCES

(1) Chheda, J. N.; Huber, G. W.; Dumesic, J. A. *Angew. Chem., Int. Ed.* **2007**, *46*, 7164−7183.
(2) Huber, G. W.; Chheda, J. N.; Barrett, C. J.; Dumesic, J. A. *Science* **2005**, *308*, 1446−1450.
(3) Huber, G. W.; Iborra, S.; Corma, A. *Chem. Rev.* **2006**, *106*, 4044−4098.
(4) Lange, J.-P.; Price, R.; Ayoub, P. M.; Louis, J.; Petrus, L.; Clarke, L.; Gosselink, H. *Angew. Chem., Int. Ed.* **2010**, *49*, 4479−4483.
(5) Geboers, J. A.; Van de Vyver, S.; Ooms, R.; Op de Beeck, B.; Jacobs, P. A.; Sels, B. F. *Catal. Sci. Technol.* **2011**, *1*, 714−726.
(6) Van de Vyver, S.; Geboers, J.; Jacobs, P. A.; Sels, B. F. *ChemCatChem* **2011**, *3*, 82−94.
(7) Van de Vyver, S.; Thomas, J.; Geboers, J.; Keyzer, S.; Smet, M.; Dehaen, W.; Jacobs, P. A.; Sels, B. F. *Energy Environ. Sci.* **2011**, *4*, 3601−3610.
(8) Climent, M. J.; Corma, A.; Iborra, S. *Green Chem.* **2011**, *13*, 520−540.
(9) Rose, M.; Palkovits, R. *Macromol. Rapid Commun.* **2011**, *32* (17), 1299−1311.
(10) Regalbuto, J. R. *Science* **2009**, *325*, 822−824.
(11) Gonzalez Maldonado, G. M.; Assary, R. S.; Dumesic, J. A.; Curtiss, L. A. *Energy Environ. Sci.* **2012**, *5*, 8990−8997.
(12) Gonzalez Maldonado, G. M.; Assary, R. S.; Dumesic, J.; Curtiss, L. A. *Energy Environ. Sci.* **2012**, *5*, 6981−6989.
(13) Bond, J. Q.; Alonso, D. M.; Wang, D.; West, R. M.; Dumesic, J. A. *Science* **2010**, *327*, 1110−1114.
(14) Serrano-Ruiz, J. C.; Wang, D.; Dumesic, J. A. *Green Chem.* **2010**, *12*, 574−577.
(15) Assary, R. S.; Curtiss, L. A. *Energy Fuels* **2012**, *26*, 1344−1352.
(16) Deng, L.; Li, J.; Lai, D.-M.; Fu, Y.; Guo, Q.-X. *Angew. Chem., Int. Ed.* **2009**, *48*, 6529−6532.
(17) Mollica, A.; Genovese, S.; Pinnen, F.; Stefanucci, A.; Curini, M.; Epifano, F. *Tetrahedron Lett.* **2012**, *53*, 890−892.
(18) Chuah, G. K.; Jaenicke, S.; Zhu, Y. Z.; Liu, S. H. *Curr. Org. Chem.* **2006**, *10*, 1639−1654.
(19) Chia, M.; Dumesic, J. A. *Chem. Commun.* **2011**, *47*, 12233−12235.
(20) Cohen, R.; Graves, C. R.; Nguyen, S. T.; Martin, J. M. L.; Ratner, M. A. *J. Am. Chem. Soc.* **2004**, *126*, 14796−14803.
(21) Campbell, E. J.; Zhou, H.; Nguyen, S. T. *Org. Lett.* **2001**, *3*, 2391−2393.
(22) Boronat, M.; Corma, A.; Renz, M. *J. Phys. Chem. B* **2006**, *110*, 21168−21174.
(23) Corma, A.; Domine, M. E.; Valencia, S. *J. Catal.* **2003**, *215*, 294−304.
(24) Boronat, M.; Concepción, P.; Corma, A.; Renz, M. *Catal. Today* **2007**, *121*, 39−44.
(25) Nikolla, E.; Roman-Leshkov, Y.; Moliner, M.; Davis, M. E. *ACS Catal.* **2011**, *1*, 408−410.
(26) Boronat, M.; Concepción, P.; Corma, A.; Renz, M.; Valencia, S. *J. Catal.* **2005**, *234*, 111−118.
(27) Assary, R. S.; Curtiss, L. A. *J. Phys. Chem. A* **2011**, *115*, 8754−8760.
(28) Assary, R. S.; Redfern, P. C.; Hammond, J. R.; Greeley, J.; Curtiss, L. A. *J. Phys. Chem. B* **2010**, *114*, 9002−9009.
(29) Assary, R. S.; Redfern, P. C.; Greeley, J.; Curtiss, L. A. *J. Phys. Chem.* **2011**, *115*, 4341−4349.
(30) Assary, R. S.; Curtiss, L. A. *ChemCatChem* **2012**, *4*, 200−205.
(31) Becke, A. D. *J. Chem. Phys.* **1993**, *98*, 5648−5652.
(32) Peterson, K. A. *J. Chem. Phys.* **2003**, *119*, 11099−11112.
(33) Roy, L. E.; Hay, P. J.; Martin, R. L. *J. Chem. Theory Comput.* **2008**, *4*, 1029−1031.
(34) Peterson, K. A.; Figgen, D.; Dolg, M.; Stoll, H. *J. Chem. Phys.* **2007**, *126*, 124101.
(35) Hay, P. J.; Wadt, W. R. *J. Chem. Phys.* **1985**, *82*, 270−283.
(36) Curtiss, L. A.; Redfern, P. C.; Raghavachari, K. *J. Chem. Phys.* **2007**, *126*, 084108.
(37) Marenich, A. V.; Cramer, C. J.; Truhlar, D. G. *J. Phys. Chem. B* **2009**, *113*, 6378−6396.
(38) Frisch, M. J.; Trucks, G. W.; Schlegel, H. B.; Scuseria, G. E.; Robb, M. A.; Cheeseman, J. R.; Scalmani, G.; Barone, V.; Mennucci, B.; Petersson, G. A.; Nakatsuji, H.; Caricato, M.; Li, X.; Hratchian, H. P.; Izmaylov, A. F.; Bloino, J.; Zheng, G.; Sonnenberg, J. L.; Hada, M.; Ehara, M.; Toyota, K.; Fukuda, R.; Hasegawa, J.; Ishida, M.; Nakajima, T.; Honda, Y.; Kitao, O.; Nakai, H.; Vreven, T.; Montgomery, J. A.; Jr., Peralta, J. E.; Ogliaro, F.; Bearpark, M.; Heyd, J. J.; Brothers, E.; Kudin, K. N.; Staroverov, V. N.; Kobayashi, R.; Normand, J.; Raghavachari, K.; Rendell, A.; Burant, J. C.; Iyengar, S. S.; Tomasi, J.; Cossi, M.; Rega, N.; Millam, J. M.; Klene, M.; Knox, J. E.; Cross, J. B.; Bakken, V.; Adamo, C.; Jaramillo, J.; Gomperts, R.; Stratmann, R. E.; Yazyev, O.; Austin, A. J.; Cammi, R.; Pomelli, C.; Ochterski, J. W.; Martin, R. L.; Morokuma, K.; Zakrzewski, V. G.; Voth, G. A.; Salvador, P.; Dannenberg, J. J.; Dapprich, S.; Daniels, A. D.; Ö. Farkas, Foresman, J. B.; Ortiz, J. V.; Cioslowski, J.; Fox, D. J. *Gaussian 09*, Rev C.01; Gaussian, Inc.: Wallingford, CT, 2009.
(39) Kozuch, S.; Martin, J. M. L. *ACS Catal.* **2012**, *2*, 2787−2794.
(40) Kozuch, S.; Shaik, S. *Acc. Chem. Res.* **2011**, *44*, 101−110.
(41) Kozuch, S.; Martin, J. M. L. *ACS Catal.* **2011**, *1*, 246−253.
(42) Kozuch, S.; Shaik, S. *J. Am. Chem. Soc.* **2006**, *128*, 3355−3365.
(43) Yu, Z.-X.; Cheong, P. H.-Y.; Liu, P.; Legault, C. Y.; Wender, P. A.; Houk, K. N. *J. Am. Chem. Soc.* **2008**, *130*, 2378−2379.
(44) Pajonk, G.; Tanany, A. *React. Kinet. Catal. Lett.* **1992**, *47*, 167−175.
(45) Wuest, J. D.; Zacharie, B. *J. Org. Chem.* **1984**, *49*, 166−168.
(46) Bermejo-Deval, R.; Assary, R. S.; Nikolla, E.; Moliner, M.; Román-Leshkov, Y.; Hwang, S.-J.; Palsdottir, A.; Silverman, D.; Lobo, R. F.; Curtiss, L. A.; Davis, M. E. *Proc. Natl. Acad. Sci. U.S.A.* **2012**, *109*, 9727−9732.
(47) Cheng, L.; Curtiss, L. A.; Assary, R. S.; Greeley, J.; Kerber, T.; Sauer, J. *J Phys. Chem. C* **2011**, *115*, 21785−21790.
(48) Kim, T.; Assary, R. S.; Marshall, C. L.; Gosztola, D. J.; Curtiss, L. A.; Stair, P. C. *ChemCatChem* **2011**, *3*, 1451−1458.
(49) Lange, J.-P.; van der Heide, E.; van Buijtenen, J.; Price, R. *ChemSusChem* **2012**, *5*, 150−166.